EUROPEAN FUSION DEVELOPMENT AGREEMENT

EFDA–JET–CP(04)07-04

H. Weisen, C. Angioni, A. Bortolon, C. Bourdelle, L. Carraro, I. Coffey, R.Dux, I. Furno, X. Garbet, L. Garzotti, C. Giroud, H. Leggate, P. Mantica, D. Mazon, D. McDonald, M.F.F. Nave, R. Neu, V. Parail, M.E. Puiatti, K. Rantamäki, J. Rapp, J. Stober, T. Tala, M. Tokar, M. Valisa, M. Valovic, J. Weiland, L. Zabeo, A. Zabolotsky, K.-D. Zastrow and JET EFDA Contributors

Anomalous Particle and Impurity Transport in JET and Implications for ITER

Anomalous Particle and Impurity Transport in JET and Implications for ITER

H. Weisen[1], C. Angioni[2], A. Bortolon[1], C. Bourdelle[4], L. Carraro[3], I. Coffey[5], R.Dux[2], I. Furno[6], X. Garbet[4], L. Garzotti[3], C. Giroud[5], H. Leggate[5], P. Mantica[7], D. Mazon[4],D. McDonald[5], M.F.F. Nave[8], R. Neu[2], V. Parail[5], M.E. Puiatti[3], K. Rantamäki[9], J. Rapp[10], J. Stober[2], T. Tala[9], M. Tokar[10], M. Valisa[3], M. Valovic[5], J. Weiland[11], L. Zabeo[5], A. Zabolotsky[1], K.-D. Zastrow[5]
and JET EFDA Contributors *

[1]Centre de Recherches en Physique des Plasmas, Association EURATOM - Confédération Suisse, EPFL, 1015 Lausanne, Switzerland
[2]IPP Garching, Germany
[3]Consorzio RFX, Padova, Italy
[4]CEA DRFC, Cadarache, France
[5]UKAEA, Abingdon, UK
[6]Los Alamos National Laboratory, USA
[7]IFP CNR Milano, Italy
[8]EURATOM-IST, Portugal
[9]EURATOM-Tekes, VTT, Finland
[10]IPP, Forschungszentrum Jülich, Germany
[11]Chalmers University, Göteborg, Sweden
** See annex of J. Pamela et al, "Overview of JET Results", (Proc. 20th IAEA Fusion Energy Conference, Vilamoura, Portugal (2004).*

Preprint of Paper to be submitted for publication in Proceedings of the
20th IAEA Conference,
(Vilamoura, Portugal 1-6 November 2004)

ABSTRACT

Results from an extensive database analysis of JET density profiles show that the density peaking factor $n_{e0}/<n_e>$ in JET H-modes increases form near *1.2* at high collisionality to around *1.5* as the plasma collisionality decreases towards the values expected for ITER. This result confirms an earlier observation on AUG. The density peaking behaviour of L modes is remarkably different from that of H modes, scaling with overall plasma shear as $(n_{e0}/<n_e>\mu l_i)$, independently of collisionality. H-mode density profiles show no shear dependence, except at the lowest collisionalities. No evidence for additional L_{Te}, L_{Ti}, T_e/T_i, β or ρ^* dependences has been obtained. Carbon and neon impurity density profiles from Charge Exchange Spectroscopy are less peaked than electron density profiles and usually flat in H modes. The possibility of heavy impurity accumulation at ITER collisionalities remains an issue. The peaking of the electron density profiles, together with the flatness of the light impurity density profiles, are favourable for fusion performance if they can be extrapolated to ignited conditions. Peaked density profiles would help to recover the fusion performance loss resulting from a possible lower-than-expected density limit in ITER.

1. DENSITY PROFILES IN ELMY H MODES

Peaked electron and fuel density profiles in reactor plasmas provide the advantage of higher reactivity, higher bootstrap fraction and stronger electron-ion coupling in the core, than obtained with flat density profiles at the same average density, albeit at the risk of impurity accumulation in the core. Most importantly, they may allow a recovery of the thermonuclear power loss, which would result if the density limit in ITER [1] is as low as half of the Greenwald density limit, as expected from a recent analysis in AUG and JET [2]. Therefore the discovery of a clear collisionality dependence of density peaking in AUG [3] H-modes called for an independent verification in JET. The theoretically important effective collisionality defined as $\nu_{eff} = \nu_{ei}/\omega_{De} \sim 3(m_i/m_e)^{1/2} \varepsilon^{3/2} \nu_{ei}/q$ (assuming $k_\theta \rho = 1/3$), where ν_{ei} is the electron collision frequency and the curvature drift frequency ω_{De} is a rough estimate of the ITG growth rate, and is therefore expected to govern both anomalous diffusion and convection [3]. The collisionality dependence of the density peaking factors for a large representative set of stationary ELMy JET H modes and 'hybrid scenario H-modes' (which have moderate to high q_{95} and low core magnetic shear) is shown in Fig.1. The density profiles were evaluated from the JET multichannel far infrared interferometer with the SVD-I inversion method [4], which uses basis function extracted from the LIDAR Thomson Scattering (TS) profiles, obtained by Singular Value Decomposition (SVD). This method greatly reduces errors in the LIDAR TS profiles, while granting consistency with interferometry. The collisionalities obtained on JET extend to below those expected for the ITER reference H-mode, indicated by a vertical line. The different symbols in Fig.1 refer to classes of internal inductance, which is a robust measure of overall magnetic shear. The same data are plotted versus l_i in Fig.2. There is no discernible dependence on l_i, except for $\nu_{eff} \leq 0.25$. This is in contrast to L-modes in DIII-D[5], TCV[6][7] and JET[8], where magnetic shear (or the peakedness of the current profile) was found to be the most important parameter, irrespective of collisionality.

The data presented here contain a great variety of conditions with $1.7\times10^{19} \le \langle ne \rangle \le 11\times10^{19} m^{-3}$, $3\times10^{-3} \le \rho^* \le 9\times10^{-3}$, $2.3 \le q_{95} \le 6.5$, $0.7 \le \beta_N \le 2.6$, $4 \le R/L_{Te}(0.5) \le 9$, $0.6 \le T_e(0.5)/T_i(0.5) \le 1.7$, $0.04 \le V_{loop} \le 0.55V$ and combinations of heating methods with $P_{nbi} \le 17MW$, $P_{rf} \le 10MW$, $P_{lhcd} \le 3MW$, including a minority of cases with substantial ICRH heating (P_{ICRH}/P_{tot} in the range 0.4-0.9 and near central deposition r/a ~ 0.3). We found no additional dependence of peaking on $\langle n_e \rangle$, nor on V_{loop}, P_{rf}/P_{tot}, β_N, ρ^*, *Te/Ti*, *LTe, or LTi*. Figs. 3&4 show the same data resolved into classes of ρ^*, and R/L_{Te}, evaluated at r/a = 0.5, illustrating this lack of further dependences. In Fig.4, to offer an alternative representation, we characterise density peaking by $R/L_n = Rdln(n_e)/dr$ at mid-radius. The results also show that the Ware pinch cannot be held responsible for density peaking at low ν_{eff}, where the lowest values of V_{loop} are obtained. The latter statement is however in contradiction with JETTO modelling of three H mode discharges, one of which was at low collisionality, and which did not require an anomalous pinch larger than the Ware pinch [9]. Figures allowing a side-by-side comparison of JET and AUG results are available from ref [10]. The peaking is slightly higher (by ~ 0.1) at $\nu_{eff} \sim 0.2$ in JET than in AUG when the evaluation of ν_{eff} is based on the average Z_{eff} derived from Visible Bremstrahlung (VB), as in Figs 1-4. JET results are however brought into full agreement with AUG when the hollow Z_{eff} profiles measured by CXS are used. Z_{eff} inferred from CXS at $r/a = 0.5$ is typically lower by a factor 1.6 than Z_{eff} from VB, shifting the ν_{eff} axis by the same factor.

It has been suggested that the peaked density profiles observed at low collisionality may result from edge gas fuelling, rather than, as proposed here, from an anomalous pinch [11]. This conclusion, obtained using the FRANTIC code, is however disputed, because it is based on neutral flux calculations based on the total D_α emission, including the divertor, which produces 90% of the D_α light in the vessel. The idea that edge, or even beam fuelling may play an important role in shaping the density profile, is at odds with experimental observations. Fig.5 shows the peaking factor versus ν_{eff} resolved by line average density. The plasma density determines the mean free path for both the neutrals originating from edge fuelling and those injected by neutral beam heating. Penetration of edge neutrals occurs by a charge exchange (CX) chain, until the chain is terminated by an ionisation. For deuterium, the average chain length is $\langle \sigma v_{CX} \rangle / \langle \sigma v_{ionisation} \rangle \sim 4$ for T_e in the keV range.

If density profiles were determined by the sole balance of the particle source and diffusion,they would only depend on the plasma density and the mixture of edge (shallow) and beam (deep) fuelling. We notice that a class of samples with $n_e \sim 4\times10^{19} m^{-3}$ (green diamonds) has peaking factors ranging from 1.3 to 1.8, in contradiction with the assumption of purely diffusive transport and a fixed source profile. We also note that in the interval $0.3 < \nu_{eff} < 0.4$, densities range from 2.5 to $6\times10^{19} m^{-3}$, yet they have the same peaking factor. Similarly, the flux of beam neutrals ($\propto P_{NBI}$) and its weight in the particle balance ($\propto P_{NBI}/\langle n_e \rangle$) vary by a factor of four in this interval, without incidence on the density peaking factor. Corroborating evidence for the absence of source effects was obtained in a recent campaign using He as the working gas, where He twins of previous D discharges were produced. He neutral penetration is strongly reduced by the low cross section for

double CX, reducing the CX chain length by a factor of ~10 with respect to deuterium. Again, if edge neutral penetration mattered, He plasmas should be much flatter than their deuterium counterparts. As seen in fig.6, the density profiles in He plasmas are, if different at all, a hint more peaked in some cases. A third element stems from the comparison of AUG and JET. If neutral penetration mattered, density profiles in the smaller AUG device would, contrary to observation, be more peaked than those in JET. Central RF heating by ICRH and ECH has been observed to flatten the density profiles in TCV [7] and AUG [13][14]. In the latter it also led to a reduction of the central heavy impurity content. Two different mechanisms may concur to produce for this phenomenon. In the first, the pinch responsible for peaking is assumed to be the Ware pinch. The flattening is then attributed to a rise of particle diffusivity proportional to the rise in core heat diffusivity resulting from the additional heat flux [13]. The second mechanism, based on drift wave turbulence theory, attributes the peaking of the density profiles to anomalous pinches and their flattening in the presence of electron heating to the destabilisation of Trapped Electron Modes (TEM), which produce a strong outward thermodiffusive particle convection counteracting the inward convection produced by the curvature pinch [3][14][15]. In the steady state density profile database presented here, there is no evidence for a significant effect of PICRH on electron density (fig.7). We note however that severe Ar impurity accumulation in Ar seeded discharges at high ν_{eff} (0.5) ~1 can lead to the development of highly peaked core density profiles and flat temperature profiles with R/L_n ~7, R/L_T ~0 for r/a <0.4 [16]. This evolution is now routinely prevented by the application of a few MW of centrally deposited ICRH. Electron heating experiments using ion Bernstein mode conversion heating in (non-seeded) H-modes have not shown any effect of the electron heating power on the density profiles. A GS2 [17] microstability analysis of these experiments, which exhibited a clear rise in $T_e(0)/\langle T_e\rangle$, but no change in $n_e(0)/\langle n_e\rangle$, showed that these plasmas remained in the ITG regime, possibly due to a lack of electron power. In the ITG regime only weak inward thermodiffusion is expected [3].

2. FUSION PERFORMANCE BENEFIT FROM PEAKED DENSITY PROFILES

The potential fusion performance benefit from peaked density profiles is considerable, as shown in fig. 8. The figure plots the ratio of the expected thermonuclear yield calculated for thermal particles, using the measured density and temperature profiles to the same ratio, assuming a flat fuel density profiles with $n_e = n_e(0.9)$ and using the approximation $R_{DT} \sim n_D n_T T_i^2$, valid for $7 < T_i < 20$keV. The symbols refer to the Greenwald number NG. The gain is nearly a factor 3, on average, for the ITER collisionality domain and nearly a factor 2 with respect to the weakly peaked plasmas at the high collisionality end. This advantage may however be entirely 'consumed''to compensate for a reduction of fusion performance, if the density limit is lower than expected. The density limit has been related to the pedestal density in JET and AUG Hmodes and has recently produced the alarming prediction that the density limit in ITER may be as low as half of the density of ITER reference H-mode [2]. If this lower limit (Borrass limit), rather than the Greenwald limit [18], applies to ITER, the loss in thermonuclear power would be at least a factor of two. This can be estimated, assuming $\langle n_e T_e\rangle$

$\propto \tau_E$""$\langle n_e \rangle$ - 0.4, as expected from ITERH.DB3 ELMy H-mode scaling [19]. The reduction will be more important still due to the unfavourable effect of the equipartition, as a result of which ions temperatures would lag significantly behind electron temperatures at low density. The gain from peaked density may compensate for the reduction of thermonuclear power that would result if the Borrass, rather than the Greenwald limit, applied to ITER. (Other caveats of low density operation, such the inability to achieve divertor detachment, are beyond the scope of this contribution).

3. DENSITY PROFILES IN L-MODES

In source-free MHD-quiescent L-mode plasmas with LHCD and with $q_0 > 1$, the density profile varies as $n_{e0} / \langle n_e \rangle$, (fig.9, coloured symbols) independently of ν_{eff}. A range of $PLHCD \leq 3.6MW$, deposited typically around $r/a \sim 0.4$, provided this scan of l_i at fixed $q_{95} \sim 8$. These experiments, reported in [8], have been reanalysed using the SVD-I method [4], showing that the peaking factor was previously underestimated by 25%. The density profiles remain peaked at $V_{loop}=0$ and negligible core particle source, as determined by KN1D [12], confirming investigations in fully current driven discharges in Tore Supra [20] and TCV [7]. As in the above H-modes, no dependence on L_{Te} was found. A GS2 analysis showed that the sign of the mode frequency is very sensitive to input parameters. This may indicate that the discharges are in a mixed ITG/TEM regime, where little or no anomalous thermodiffusion, and hence non L_{Te} dependence, is expected [14]. The l_i dependence is consistent with an anomalous pinch resulting from Turbulent EquiPartition [5]. Transport simulations using JETTO on a small number of L-mode discharges (not part of the above LHCD set) have also concluded that an anomalous pinch is present in L-modes [9].

4. IMPURITY DENSITY PROFILES AND ACCUMULATION

Peaked density profiles, as found in many L-modes and in H-modes at low collisionality, raise the concern of neoclassical impurity accumulation, especially of the proposed ITER divertor material tungsten. Radial neoclassical impurity convection results from an inward term due to the main ion density gradient and an ion temperature gradient contribution which depends on the overall ion collisionality ν^*_{ib} (b stands for the background ions) [21] and may partly or fully counteract ('screen') the inward convection if $\nu^*_{ib}<1$, as expected for the ITER reference H-mode ($\nu^*_{ib} \sim 0.4$ at r/a=0.5). For a heavy impurity in a hydrogen plasma with a typical light impurity concentration, the relevant background collisionality is dominated by that of the light impurities. In the current dataset, the possibility of some screening is limited to the lower end of the ν_{eff} range where $\nu^*_{i6} \sim 1$ at r/a=0.5, calculated on the basis of the plasma deuterium and carbon content. At $\nu_{eff}>0.7$, $\nu^*_{i6}>3$ (typically), and the ion temperature gradient somewhat reinforces the inward convection [21]. Recent calculations using the Weiland model also show that anomalous inward convection, which scales as 1/Z, is lower for carbon than for deuterium.

Fig.9 shows that in L-mode, the carbon density profile from CXS, is significantly less peaked than the electron density profile. In H-mode, carbon density profiles are rather flat or slightly hollow, as seen for three examples with different collisionalities in fig.10. As a result, carbon concentration,

n_c/n_e, profiles are hollow inside $r/a\sim0.7$, especially at low collisionality, when density profiles are most peaked (fig.11). Neon gas puff experiments in hybrid H-modes have provided transport coefficients such that v/D are similar to those of intrinsic carbon ($v_i/D_i=d/n n_i/dr$ in source free regions in steady state) [22]. The slight hollowness of light impurity density profiles exceeds theoretical expectations ($V\propto 1/Z$) and raises the question wether NC ion temperature screening may contribute. This appears to be impossible in view of the high diffusion coefficients ($D\sim1\text{-}4m^2/s$, two orders of magnitude beyond NC) obtained for Ne and Ar in the confinement region [22]. The complex structure and large magnitude of the convective velocity in impurity transport simulations [22][23] is also at odds with NC theory.

Ar seeding has been used in high density discharges to simultaneously obtain high density, good confinement and an edge radiation belt. Ar in these H-mode discharges, which had $\nu_{eff} > 0.6$ and $\nu^*_{i6}>3$, was prone to a process of slow, but severe, central accumulation, often developing highly peaked electron and Ar densities and high core radiation losses, especially at low triangularity [16][23][24]. These radiation losses and lack of net heating power in the core led to core shear reversal with $q_{min}>1$ and the suppression of sawteeth, thereby worsening the accumulation. A few MW of central ICRH was sufficient for maintaining sawteeth (or sometimes a (1,1) MHD mode), for flattening the core electron and Ar density profiles, allowing access to stationary high performance discharges [16].

Results for laser ablated, transient Ni injection are shown in fig.12. The figure shows peaking factors extrapolated to steady state, as deduced from X-ray measurements and modelled using an ionisation equilibrium code to provide radially resolved transport parameters. Steadystate profiles were then reconstructed from v(r) and D(r), assuming a constant edge source. Some of these are considerably more peaked than the electron density profiles, with most of the impurities concentrated near the magnetic axis, inside $r/a<0.25$, while outside this region, Ni concentrations were constant. In the confinement zone, Ni diffusion coefficients in H-mode ($1<D<4m^2/s$, depending on the discharge) and L-mode ($2<D<7m^2/s$) were clearly anomalous and much lower towards the axis and near the edge in H-mode. These observations, as others (e.g.[25]), support the view that in the core, where anomalous transport is low in the absence of sawteeth, heavy impurity transport is dominated by NC processes. In particular, the observation that Ni profiles can be strongly peaked in the core at low ν_{eff}, reinforces our concerns about tungsten accumulation in ITER.

5. DISCUSSION AND SUMMARY

The above observations pose welcome constraints on the theoretical understanding and on ongoing modelling efforts. Some observations can be related to existing theories. The ν_{eff} dependence in H-modes, which are largely in the ITG regime, is in agreement with fluid modelling [3]. Positive shear L-modes and H-modes at low ν_{eff} have profiles which are consistent with Turbulent EquiPartition [5], as expected from purely diffusive transport of trapped particles in poloidal flux space, i.e $\Delta N/\Delta\Psi$ ~constant (where ΔN is the number of particles in the interval $\Delta\Psi$) over most of the cross section. A theoretical difficulty is the existence of peaked density profiles at high ν_{eff} in L-modes, while, for

high values of ν_{eff}, Hmode profiles are much flatter. Another difficulty is to understand why there is no evidence for a shear dependence for H-modes at $\nu_{eff} > 0.2$, despite the expectance that the curvature pinch is the dominant convective mechanism when ITG's dominate [14].

It seems reasonable to assume that the differences are somehow linked to the nature of the underlying turbulence (ITG or TEM). The fundamental difference between L and H-modes is the edge pedestal, which appears to lead to flatter core density profiles, which is stabilising TEMs and destabilising for ITGs. At $\nu_{eff} < 0.2$, however, the significant density gradient in Hmode would reduce ITG growth rates and contribute to destabilising TEMs, which may explain why a shear dependence similar to that of L-modes is observed. (Recent observations in TCV and AUG also suggest that the domains where scaling with ν_{eff}, respectively shear, is observed do not coincide neatly with the H and L-mode regimes). The L-modes reported above appear to be in a mixed ITG/TEM regime, not however dominated by TEMs, as can be produced in devices equipped with high power electron heating such as TCV and AUG, where density profiles have been observed to flatten in response to central electron heating [13][20][14].

The agreement between JET and AUG, together with the lack of significant dependencies on dimensionless parameters other than ν_{eff} (and l_i at the lowest ν_{eff}), suggests that an extrapolation to ITER H-modes should be possible. Assuming otherwise similar conditions, we expect $n_{e0}\,D/\langle n_e \rangle \approx 1.5 \pm 0.2$ for the collisionality of the ITER reference H-mode, corresponding to $R/L_n \approx 4 \pm 1$ at mid-radius. We expect this prediction to apply to the initial, non-active phase of operation when hydrogen or helium will be used as working gases. This peaking would also imply a boost in thermonuclear fusion yield of nearly a factor of 3 over a flat density profile with density clamped at r/a=0.9. This may compensate for a possible lower density limit in ITER [2]. Extrapolation to ignited conditions is uncertain, because the large electron heating power deposited in the core by α-particles may destabilise TEMs, leading to flatter density profiles. A positive effect may however be a concomitant reduction of the core impurity content. The amount of net electron heating and their effect on TEMs will however be reduced by electron-ion coupling, for which smaller devices with high local electron heating power densities are not necessarily representative. The non-observation, so far, of density flattening in JET should not be taken as an indication that the phenomenon disappears in large enough devices, since it may be also due to a lack of electron heating power available in JET. The issue calls for dedicated experiments at low ν_{eff}, where the central electron heating is tailored as to emulate the net electron heating profile in ITER.

ACKNOWLEDGEMENT

This work was partly supported by the Swiss *Fonds National de la Recherche Scientifique*.

REFERENCES

[1]. V. MUKHOVATOV et al, Plasma Phys. Contr. Fusion **45** (2003) A235

[2]. K. BORRASS et al., Nuclear Fusion **44** (2004) 752

[3]. C. ANGIONI et al, Phys. Rev. Lett. **90** (2003) 205003

[4]. I. FURNO et al, Plasma Phys. Contr. Fusion **46** (2004), accepted, due Dec. 2004
[5]. D.R. BAKER et al, Nuclear Fusion **40** (2000) 1003
[6]. H. WEISEN et al, Nuclear Fusion **42** (2002) 136
[7]. A. ZABOLOTSKY et al, Plasma Phys. Contr. Fusion **45** (2003) 735
[8]. H. WEISEN et al, Plasma Phys. Contr. Fusion **46** (2004) 751
[9]. L. GARZOTTI et al, Nucl. Fusion **43** (2003) 1829
[10]. X. GARBET et al (2004), accepted for Plasma Phys. Contr. Fusion (invited EPS 2004)
[11]. M. VALOVIC et al, 2004, accepted for Plasma Phys. Contr. Fusion
[12]. B. LABOMBARD, MIT PSFC report PSFC-RR-01-03 (2001)
[13]. J. STOBER et al., Nuclear Fusion **41** (2001) 1535
[14]. C. ANGIONI et al, Nuclear Fusion **44** (2004) 827
[15]. X. GARBET et al, Phys. Rev. Lett. **91** (2003) 35001
[16]. M.F.F. NAVE et al, Nuclear Fusion **43** (2003) 1204
[17]. M. KOTSCHENREUTHER et al, Comput. Phys. Commun. **88** (1995) 128
[18]. M. GREENWALD et al, Nucl. Fusion **28** (1988) 2199
[19]. ITER EXPERT GROUPS et al, ITER Physics Basis, chap 2, Nucl. Fusion **39** (1999) 2175
[20]. G.T. HOANG et al, Phys. Rev. Lett. **90** (2003) 155002
[21]. S.P. HIRSHMAN AND D.J. SIGMAR, Nuclear Fusion **21** (1981) 1079
[22]. C. GIROUD et al, 31st EPS on Plasma Physics, London (2004) P1.144
[23]. M.E. PUIATTI et al, Plasma Phys. Contr. Fusion **45** (2003) 2011
[24]. M.Z. TOKAR et al, Nucl. Fusion **37** (1997) 1691
[25]. R. DUX, Fusion Science and Technology **44** (2003) FST-11 276903

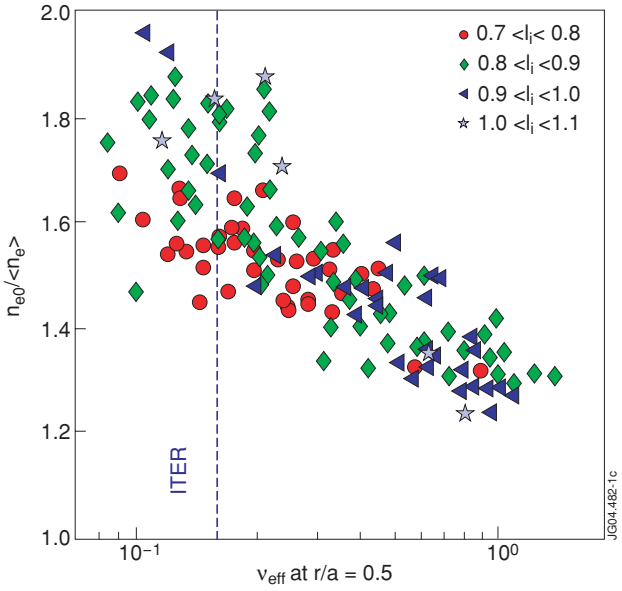

Figure 1: Density peaking factor in H-mode versus ν_{eff} at r/a=0.5. Symbols: classes of internal inductance l_i.

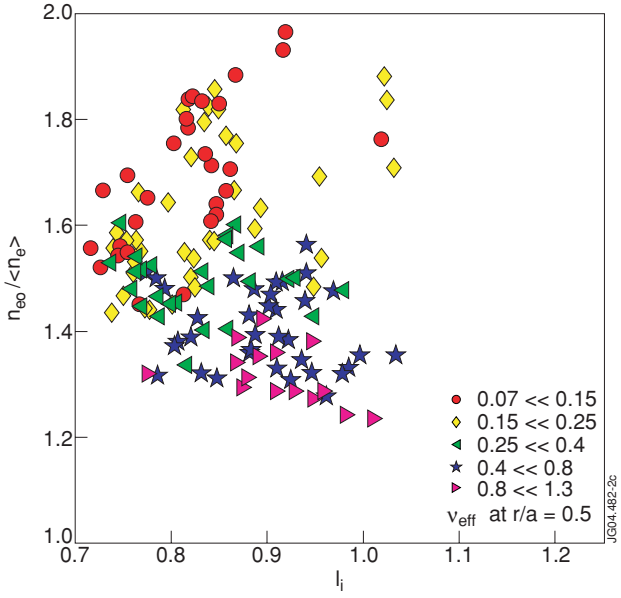

Figure 2: Peaking factor in H-mode versus l_i, resolved by classes of effective collisionality ν_{eff}.

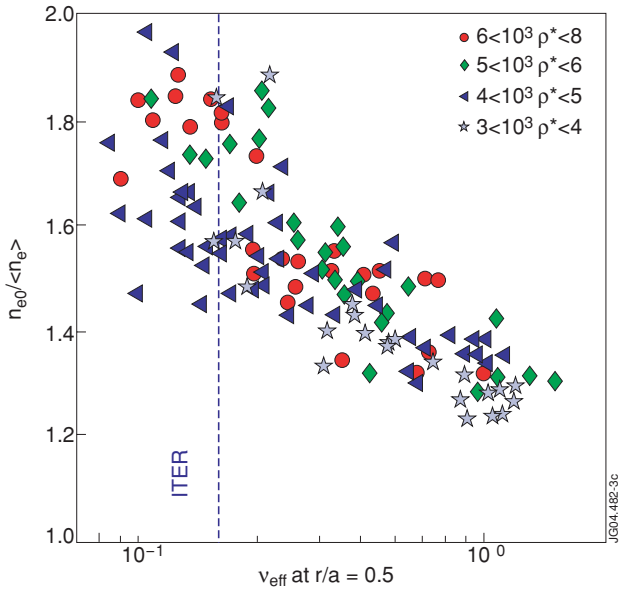

Figure 3: Peaking factor in H-mode versus ν_{eff}, resolved by classes of ρ evaluated at r/a=0.5.*

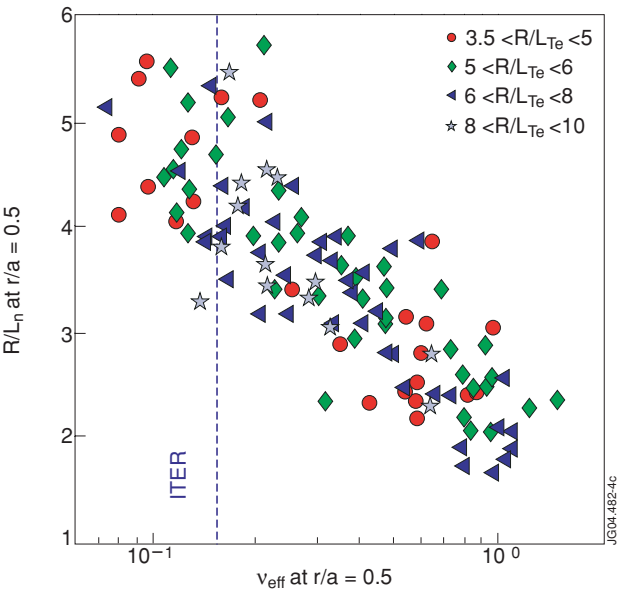

Figure 4: Normalised electron density gradient in Hmode at r/a=0.5 versus ν_{eff}, resolved by classes of electron temperature gradient.

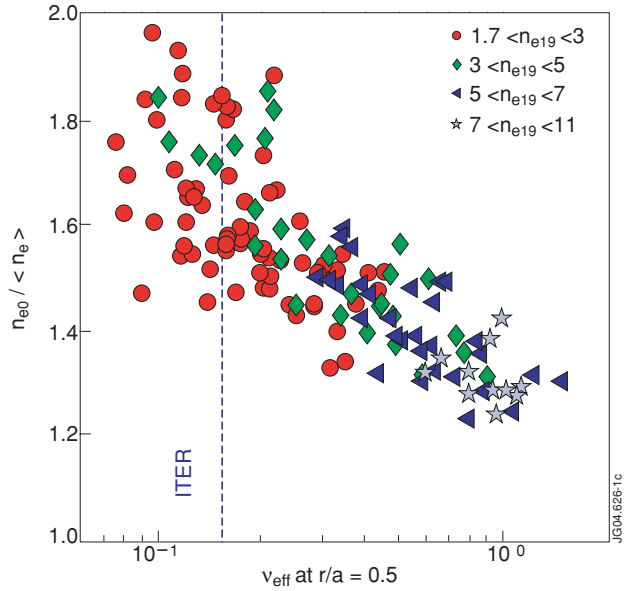

Figure 5: As fig. 3, resolved by line average density.

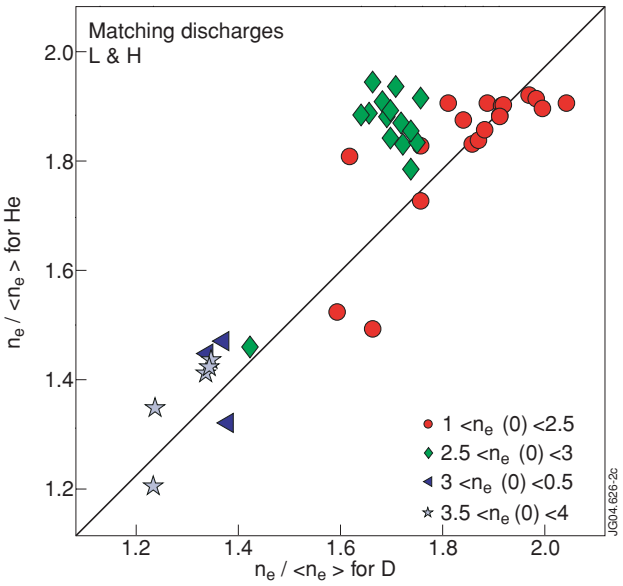

Figure 6: Comparison of peaking factors in deuterium plasmas with their counterparts in He.

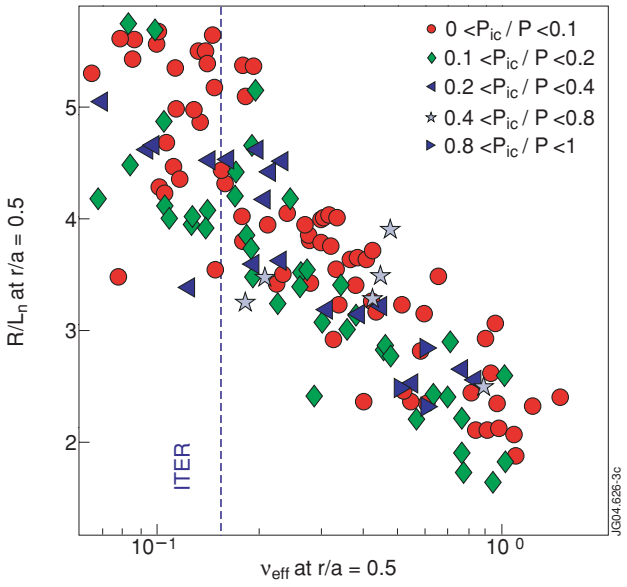

Figure 7: H-mode density gradients resolved by fraction of ICRH heating power.

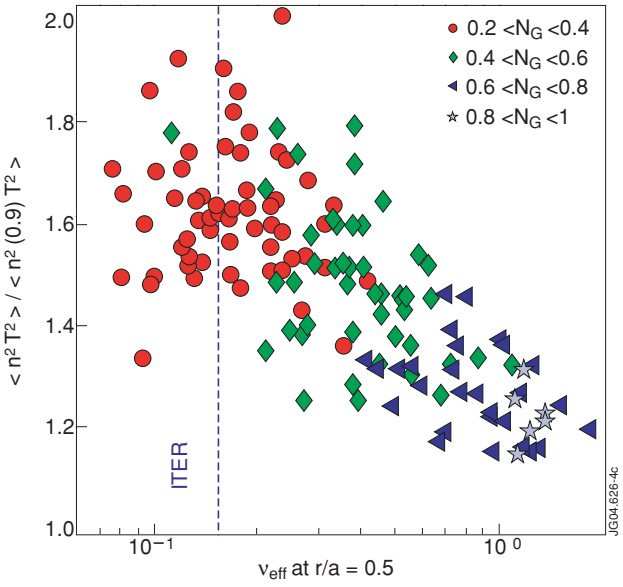

Figure 8: Increase of expected thermonuclear yield over plasma with flat density profile clamped at ne(0.9).

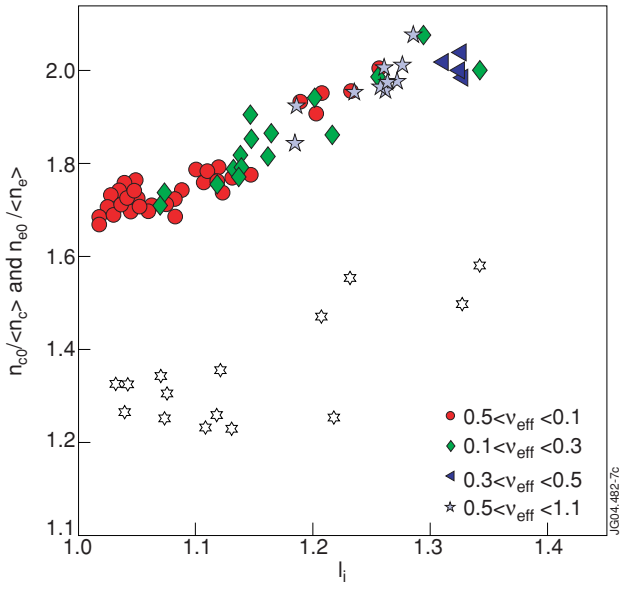

Figure 9: Density peaking in LHCD L-modes versus internal inductance, resolved by effective collisionality at r/a=0.5. Stars: Carbon impurities.

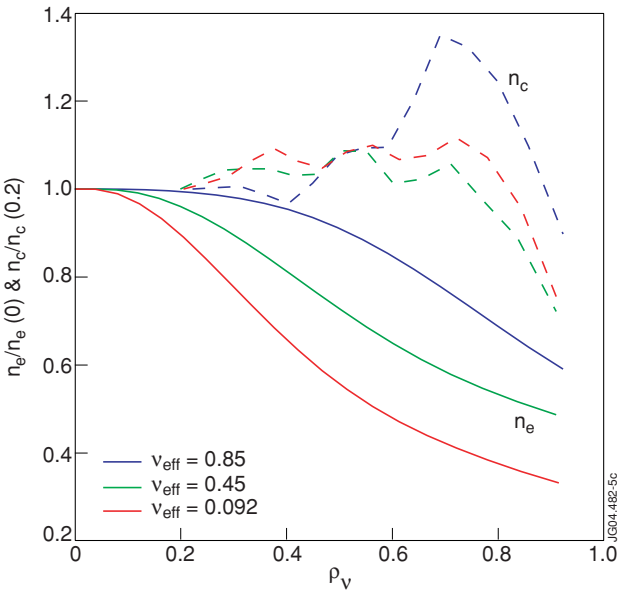

Figure 10: Normalised H-mode electron (-) and carbon impurity density (--) profiles for three different ν_{eff} and q_{95}~3.

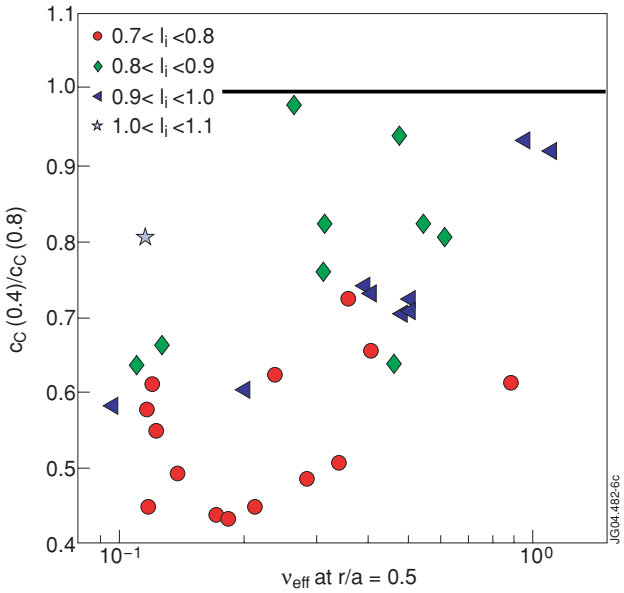

Figure 11: Ratio of carbon concentrations at r/a=0.4 and 0.8 as function of ν_{eff} in H-modes.

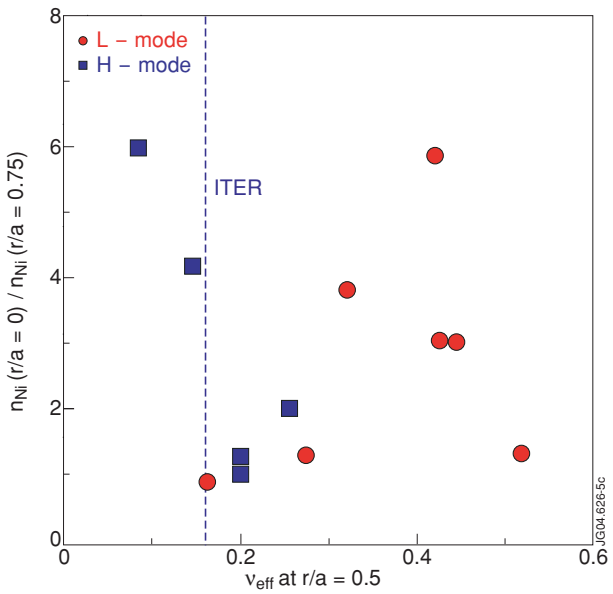

Figure 12: Peaking of laser-ablated Nickel density profiles (transient).